

We are IntechOpen, the world's leading publisher of Open Access books Built by scientists, for scientists

5,300

Open access books available

130,000

International authors and editors

155M

Downloads

Our authors are among the

154

Countries delivered to

TOP 1%

most cited scientists

12.2%

Contributors from top 500 universities



WEB OF SCIENCE™

Selection of our books indexed in the Book Citation Index
in Web of Science™ Core Collection (BKCI)

Interested in publishing with us?
Contact book.department@intechopen.com

Numbers displayed above are based on latest data collected.
For more information visit www.intechopen.com



Chapter

Techno-Economic Optimization and Benchmarking of a Solar-Only Powered Combined Cycle with High-Temperature TES Upstream the Gas Turbine

Fritz Zaversky, Iñigo Les, Marcelino Sánchez, Benoît Valentin, Jean-Florian Brau, Frédéric Siros, Jonathon McGuire and Flavien Berard

Abstract

This work presents a techno-economic parametric study of an innovative central receiver solar thermal power plant layout that applies the combined cycle (CC) as thermodynamic power cycle and a multi-tower solar field configuration together with open volumetric air receivers (OVARs). The topping gas turbine (GT) is powered by an air–air heat exchanger (two heat exchanger trains in the case of reheat). In order to provide dispatchability, a high-temperature thermocline TES system is placed upstream the gas turbine. The aim is threefold, (i) investigating whether the multi-tower concept has a techno-economic advantage with respect to conventional single-tower central receiver plants, (ii) indicating the techno-economic optimum power plant configuration, and (iii) benchmarking the techno-economic optimum of the CC plant against that of a conventional single-cycle Rankine steam plant with the same receiver and TES technology. It is concluded that the multi-tower configuration has a techno-economic advantage with respect to the conventional single-tower arrangement above a total nominal solar power level of about 150 MW. However, the benchmarking of the CC against a Rankine single-cycle power plant layout shows that the CC configuration has despite its higher solar-to-electric conversion efficiency a higher LCOE. The gain in electricity yield is not enough to outweigh the higher investment costs of the more complex CC plant layout.

Keywords: concentrated solar power, solar combined cycle, multi-tower central receiver, open volumetric air receiver (OVAR)

1. Introduction

Solar thermal power, also known as concentrated solar power (CSP) or solar thermal electricity (STE), can be considered as a highly promising technology when

it comes to dispatchable and thus grid-friendly supply of renewable electricity. This is due to the possibility of thermal energy storage (TES), the key advantage over other renewable technologies (such as wind or photovoltaic), which enables the decoupling between solar energy collection and electricity production. Given the abundant amount of solar power available for terrestrial solar collectors (85 PW) [1], which exceeds the current world's power demand (15 TW) several thousand times [1], CSP is a highly promising and flexible alternative to conventional fossil-fuel technologies, setting new standards in terms of environmental impact, sustainability, safety, and thus quality of life.

Until recently, the cost of electricity generation for CSP (≈ 14 c€/kWh [2]) has been clearly above conventional technology and other renewables (wind and photovoltaic reach 6 c€/kWh on average [2]). Nevertheless, considering latest bids, cost targets as low as 7 c\$/kWh [3] seem to be realistic for mature CSP technology. However, rather than comparing the pure cost, one should compare the true value of CSP for grid operation and capacity [2] when considering an increasing fraction of not-dispatchable renewables. It is important to note that CSP should not be seen as a competing technology with photovoltaic or wind power. It should rather be seen as an enabling technology of not-dispatchable renewable power generation, as a key feature of CSP is its cheap thermal energy storage, guaranteeing dispatchability.

This work focuses on central receiver CSP plants [4] analyzing the economic competitiveness of the combined cycle (topping GT plus bottoming steam Rankine) with respect to conventional single-cycle Rankine steam technology. The combined cycle technology [5–7] is well known from conventional fossil-fired power generation, reaching cycle efficiencies exceeding 60% on a lower heating value basis [8]. However, these best of class efficiencies are obtained with latest fossil-fired gas turbine (GT) technology, achieving turbine inlet temperatures (TITs) of up to $\approx 1500^\circ\text{C}$. It is clear that such high TITs can only be achieved with (i) internal combustion and (ii) turbine blade cooling and single-crystal superalloy turbine blades, furthermore coated with low conductivity ceramics. For the application of solar combined cycles, the TIT has to be significantly lower for two reasons: (i) the optimum receiver operating temperature (\approx TIT) that optimizes solar-to-electric conversion efficiency is a function of the receiver's thermal efficiency and tends to be at around 1000°C [9, 10] depending on the receiver technology; (ii) for solar combined cycles, the concept of externally heated gas turbines [11] has to be exploited, which limits the maximum achievable TIT to lower values (≈ 900 – 1000°C) in any case. Additionally, cheaper designs for the turbine should be used in order to keep costs down, i.e., uncooled turbine blades, which should be achievable with expected optimum receiver working temperatures of $\approx 1000^\circ\text{C}$ [9]. Furthermore, advanced gas turbine architectures [12] such as reheat will be necessary to achieve good GT efficiencies, despite low TITs. Reheated gas turbines have already been treated in previous works. The main motivations are (i) to keep the average temperature of heat supply high and (ii) to introduce an additional flexibility regarding turbine exit temperature (TET) (the heat recovery steam generator inlet temperature), despite high compressor pressure ratios [13]. In particular, the expansion ratio of the second turbine stage can be specifically designed, so that the resulting TET optimizes the overall combined cycle performance. Note that the higher the heat recovery steam generator's inlet temperature is, the higher are the conversion efficiency and power output of the bottoming cycle and vice versa.

It is clear that the solar receiver unit is the key component of a solar-powered combined cycle plant, since it is of utmost importance to achieve very good solar receiver efficiencies at highest operating temperatures ($\approx 1000^\circ\text{C}$). So far, pressurized air receivers have been the design principle for solar-powered gas turbines,

since the solar receiver has to provide heat to a pressurized air stream coming from the gas turbine's compressor. Several previous research projects have already endeavored to design such a demanding component, which has to operate under very high solar flux ($\approx 0.5\text{--}1\text{ MW/m}^2$), at high temperatures ($> 900^\circ\text{C}$), and in addition at pressures over 6 bar. The first developments started in the 1980's with metallic and ceramic tubular designs [14]. This approach showed however durability issues and also low efficiencies because of the low heat transfer coefficient of air. Therefore, pressurized volumetric receivers [15] appeared to be a promising alternative as they increased the heat transfer area. However, durability issues and size limitations of the needed quartz glass window have hindered their commercial application so far. For this reason, the idea of pressurized tubular or opaque-heat-exchanger-type receivers was revisited by several research groups. For example, Grange et al. [16] investigated a modular metallic absorber located at the back of a cavity. The maximum air outlet temperature was reported to be 750°C . Korzynietz et al. [17] developed a pre-commercial scale metallic tubular cavity receiver achieving thermal efficiencies between 71.3 and 78.1% at the maximum air outlet temperature of 800°C .

However, although dispatchability is the key advantage of CSP (due to cost-effective thermal energy storage) and its best argument to justify higher costs than PV or wind energy, only a few works have covered the integration of high-temperature TES upstream the solar combined cycle. Since only pressurized receivers have been applied so far in the context of solar-powered combined cycles, previous works have proposed the application of pressurized regenerative TES systems [16, 18], which have clear limitations regarding cost-effective large-scale deployment.

The aim of this work is therefore to present an innovative plant layout (as shown in **Figure 1**) that not only avoids the design challenges related to pressurized receivers but also allows the integration of an atmospheric air-based high-temperature TES system upstream the combined cycle. In particular, this work proposes the application of the open volumetric air receiver technology [15], which has already been demonstrated successfully at pre-commercial scale [19], in

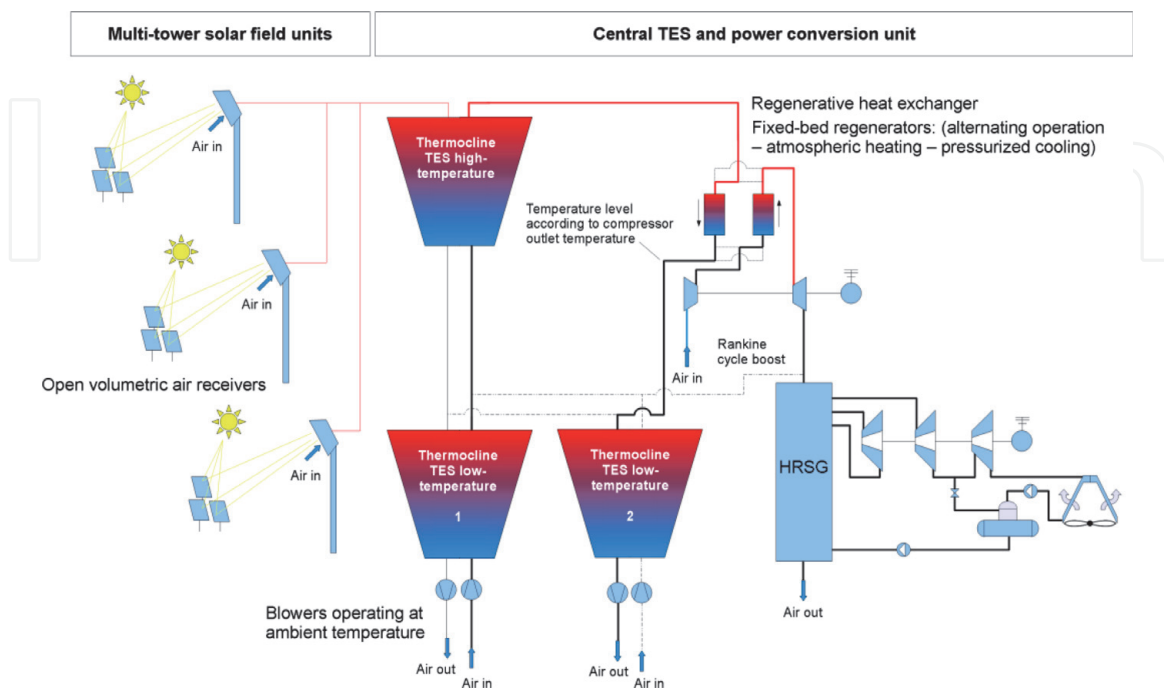


Figure 1. Solar-powered combined cycle scheme with open volumetric air receiver and high-temperature TES (without reheat in the Brayton cycle). The low-temperature TES enables regenerative use of return air heat.

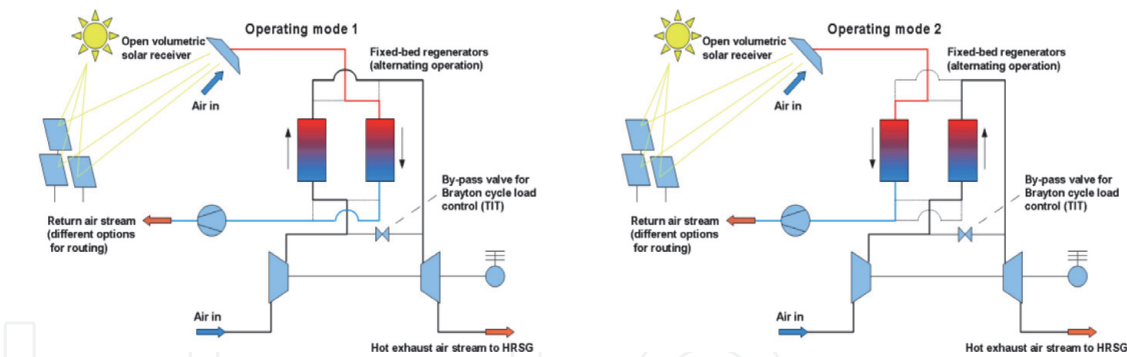


Figure 2.
Innovative coupling of open volumetric air receiver and Brayton cycle.

combination with a regenerative system working in alternating modes (atmospheric heating, pressurized cooling; see **Figure 2**) in order to power a solar-only combined cycle. This approach decouples the high-temperature and the high heat flux part (solar receiver) from the high pressure part (compressed air stream of the Brayton cycle) via an air–air regenerative heat exchanger. Thus, upstream the combined cycle, the well-proven and relatively cheap regenerator-type heat storage known from the so-called Cowper Stoves [7, 20, 21] can be used. The regenerative matrix consists of refractory bricks with channels in between where the gas is flowing, transferring heat to the bricks or vice versa [20]. This type of regenerative heat storage has already been demonstrated successfully at pilot plants [22–24] for the application of CSP. The big advantages of this technology are (i) a simple design with very low technological risk and (ii) low costs ($\approx 17 \text{ €/kWh}_{\text{th}}$ [25]).

The temperature level of the “cold” return air stream leaving the air–air heat exchange system is a function of compressor outlet temperature (i.e., compressor pressure ratio and ambient temperature) and the exit temperature of the first turbine stage, in the case of reheat. The resulting air-return temperature level is too high for efficient blower operation and the recirculation to the high-temperature TES or the receiver is thus not feasible. A low-temperature air/rock thermocline TES is thus proposed in order to reuse the return air heat in regenerative manner. In order to keep air transport parasitic power consumption acceptable, the operating temperature of the blower should be kept at ambient temperature level.

A related work [10] has shown that the thermodynamic performance of this power plant layout, having an effective mean solar flux concentration ratio of 500, optimizes at a receiver outlet temperature ($\approx \text{TIT}$) of about 1050°C and a Brayton cycle pressure ratio of 14 (reheat ratio $K=0.75$), resulting in about 29.6% peak solar-to-electric conversion efficiency. The present work continues the research, focusing on the techno-economic optimization and benchmarking of the proposed power plant layout. The aim is threefold, (i) investigating whether the multi-tower concept has a techno-economic advantage with respect to conventional single-tower central receiver plants, (ii) indicating the techno-economic optimum of the power plant size (the number of towers, solar field size, solar multiple, and hours of TES), and (iii) benchmarking the techno-economic optimum of the solar-powered combined cycle plant against that of a conventional single-cycle Rankine steam plant [22] with the same receiver (but lower operating temperature, $\approx 800^\circ\text{C}$) and TES technology (see **Figure 3**).

1.1 Advantages and limitations of air as heat transfer fluid (HTF)

Probably the most important advantage of air as HTF is that it has no temperature limit. Thus, overheating and freezing are no issue, in contrast to the application

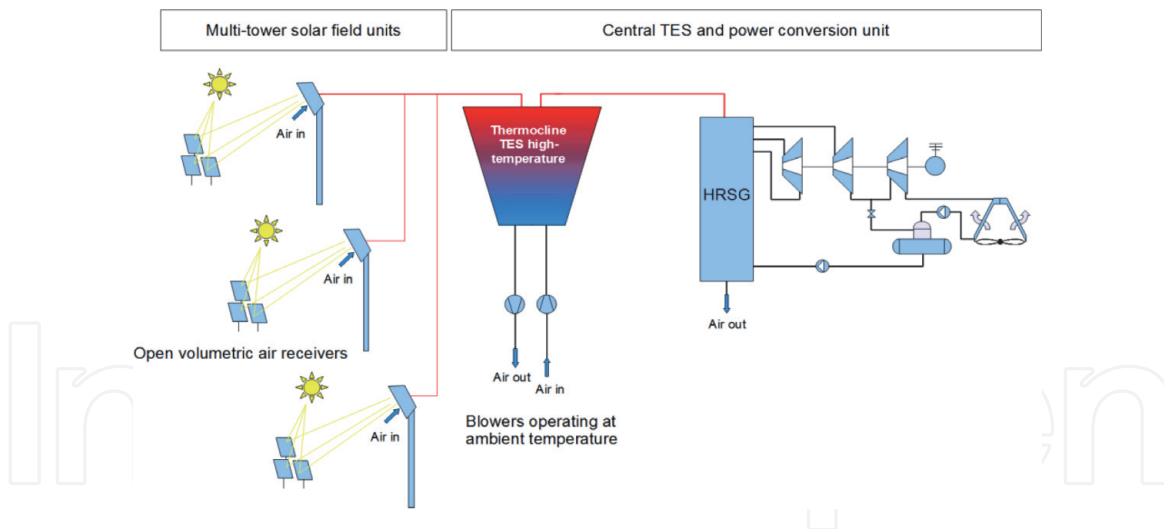


Figure 3.
Single cycle Rankine scheme—Optimum receiver outlet temperature is 800°C.

of molten salts or thermal oil. For this reason, no expensive heat-tracing equipment is needed, and furthermore the application of air as HTF allows the implementation of advanced power cycles such as the combined cycle (topping gas turbine and bottoming Rankine cycle), which requires temperatures of cycle heat input in the range between 800 and 1100°C (the optimum gas turbine inlet temperature depends on the receiver efficiency).

The second advantage is that air is freely available and obviously nontoxic to human kind and nature. Thus, no investment or cost of replacement during power plant life time must be considered. However, it may be necessary to thoroughly clean (filter) the air after recirculation in the heat transport circuit before its release to the ambient, as particulate matter coming from piping material, especially from high-temperature insulation fibers, must not be released to the atmosphere. If released it would represent an important health hazard.

The third advantage is that very cost-effective thermal energy storage technology is available when using atmospheric air as HTF. Here, the well-proven and relatively cheap regenerator-type heat storage known from the so-called Cowper stoves [20, 21], which are applied together with blast furnaces, can be used. These high-temperature regenerators work at temperatures of up to 1250°C [20] providing hot gas at constant temperature to the furnace. The outlet temperature of the regenerators is typically controlled by adding a variable flow of cold air at the outlet [21]. The regenerative matrix consists of refractory bricks with channels in between where the gas is flowing, transferring heat to the bricks or vice versa [20]. This type of regenerative heat storage has already been demonstrated successfully at pilot plants [22, 23] for the application of CSP. The big advantages of this technology are (i) a simple design with very low technological risk and (ii) low costs [25]. Possible storage vessel core geometries are packed beds, consisting of spheres or broken particles, stacks of plates, perforated bricks, or extruded shapes [26]. In packed beds, the efficiency of thermal energy storage depends on the heat transfer between the air and the filler material, as well as on the reached stratification or thermocline. Good heat transfer and limited heat transport within the solid storage media that enhances thermal stratification is reached by porous structures [27]. A truncated conical shape of the container, coupled with subterranean location, may alleviate problems such as rock fracture and tank deformation. The inclined walls reduce the mechanical constraints by guiding the rocks upwards during thermal expansion [24].

As indicated above, air as HTF has important advantages, which however are limited by the fact that air is not very suitable when it comes to heat transport over longer distances and heat transfer, especially at atmospheric pressure. The heat transport issue of atmospheric air circuits is caused by the very low density of air at high temperatures ($\approx 0.28 \text{ kg/m}^3$ at 1000°C), which leads to high flow velocity and thus elevated pressure drops (high blower power consumption). Therefore, the air piping system must provide sufficiently large flow cross sections in order to keep flow velocity in the order of magnitude of 15–30 m/s. This requirement leads to large diameter piping that needs to be insulated internally as high-temperature alloys are too expensive.

However, not only the associated pressure drop (parasitic power consumption) is an issue when applying air as HTF. Also thermal losses and thermal inertia effects are important design aspects for air-based CSP plants.

All the abovementioned disadvantages have to be properly addressed for the scale-up to commercial size of atmospheric air-based CSP plants. As described later on, the upscaling of CSP plants is important, as specific power cycle costs (USD/kWe) are significantly lower when moving to higher nominal power output. Therefore, CSP plants have increased in size recently. When upscaling a CSP plant to several hundreds of MWe, several heliostat fields and receivers may be needed to provide heat to the same power cycle: in such a case, the applied HTF needs to transport heat over very long distances (1–2 km). However, when applying air as HTF, thermal losses as well as thermal inertia effects (because of cooldown at night) are a major hurdle to its large-scale commercial implementation. In the following, the performance of an 800 m high-temperature air duct will be given, transporting the thermal power delivered by a 51 MWth heliostat field (Case C, **Table 1**).

Assuming a receiver outlet temperature of 1000°C and a corresponding receiver efficiency of 0.754 results in a nominal air mass flow of about 36 kg/s. For the design of the needed piping system, several techno-economic considerations need to be taken into account. The piping inner diameter defines the flow cross section and the outer circumferential surface area which needs to be thermally insulated. The ratio of flow cross area to the outer surface area (that defines piping and insulation material mass) becomes higher for larger inner diameters. Therefore, the inner diameter should be chosen as big as possible, i.e., considering manufacturing and structural strength limitations. In principle, circular duct geometry is the better choice as outer surface area per square meter of flow cross section is lower than in the case of rectangular cross section.

For the specific example, an inner piping diameter of 3 m has been chosen. The default thickness and thermal conductivity of the thermal insulation are 0.6 m and 0.035 W/(m K) , respectively. The heat transfer coefficient between ambient air and outer pipe surface is assumed to be $\approx 10 \text{ W/(m}^2 \text{ K)}$. For the default case (Case 1 in **Table 2**), the given settings result in a flow velocity of 19 m/s and a total pressure drop [28] of about 0.22 kPa (800 m total piping length). The thermal loss to the ambient air (at 25°C) causes a temperature reduction of about 12°C , down to 988°C . As **Table 2** further indicates, when increasing the mass flow rate, the temperature drop reduces; however pressure drop more than doubles. Thus, one measure to reduce the temperature reduction is to increase mass flow rate, however, with the cost of higher parasitic power consumption. Obviously, since the thermal losses remain practically constant (the same temperature difference to ambient and overall heat transfer coefficient remains almost constant), a higher mass flow rate translates to lower temperature difference in the air flow. The second measure to reduce temperature drop is to increase insulation thickness (see **Table 3**), which however is very expensive.

| | Solar field power classes | | | | |
|-------------------------------|---|--|--|--|--|
| | A | B | C | D | E |
| Nominal solar power (MW) | 5.666 MW (North) | 17 MW (North) | 51 MW (North) | 153 MW (Surround) | 459 MW (Surround) |
| Mirror area (m ²) | 7248 | 21,960 | 68,560 | 221,640 | 710,240 |
| Annual optical efficiency (-) | 0.7782 | 0.7644 | 0.7368 | 0.6827 | 0.6486 |
| Field diameter (m) | 240 | 380 | 750 | 1300 | 2400 |
| Tower height (m) | 50 | 80 | 100 | 150 | 200 |
| Nominal solar power (MW) | Tower configurations analyzed and corresponding LCOE (c\$/kWh (CC)) (c\$/kWh (RC)) | | | | |
| 17 | 3 A (CC = 19) (RC = 20.4) | 1 B (CC = 16.7) (RC = 17.4) | — | — | — |
| 34 | 6 A (CC = 17.7) (RC = 18.2) | 2 B (CC = 15.6) (RC = 15.7) | — | — | — |
| 51 | 9 A (CC = 17) (RC = 16.9) | 3 B (CC = 15.1) (RC = 14.7) | 1 C (CC = 13.8) (RC = 13.1) | — | — |
| 102 | — | 6 B (CC = 14.1) (RC = 13.6) | 2 C (CC = 13.6) (RC = 13) | — | — |
| 153 | — | 9 B (CC = 13.6) (RC = 12.5) | 3 C (CC = 13.4) (RC = 12.5) | 1 D (CC = 13.8) (RC = 12.6) | — |
| 204 | — | — | 4 C (CC = 13.2) (RC = 11.8) | — | — |
| 306 | — | — | 6 C (CC = 12.6) (RC = 11.5) | 2 D (CC = 14.6) (RC = 13.7) | — |
| 459 | — | — | 9 C (CC = 12.9) (RC = 12.3) | 3 D (CC = 14.4) (RC = 14) | 1 E (CC = 14.7) (RC = 14.2) |
| 612 | — | — | — | 4 D (CC = 14.5) (RC = 14.1) | — |

Table 1.
 Solar field base modules and multi-/single-tower configurations analyzed.

This analysis shows that a temperature drop of $\approx 10^\circ\text{C}$ is a reasonable assumption for the multi-tower concepts analyzed later on.

Last but not the least, the second issue, as mentioned above, is related to low heat transfer performance when applying air as HTF. For this reason, heat exchangers need to have a very large area of heat transfer in order to counterbalance this drawback. This is the reason why heat recovery steam generators of combined cycle plants are very bulky and represent an important share of the power block's CAPEX. The same holds for the air-air heat exchanger that is needed for the CAPTure power plant layout (see **Figure 1**). Here, the motivation is to reduce cost

| | Case 1 | Case 2 | Case 3 | Case 4 | Case 5 | Case 6 |
|---|--------|--------|--------|--------|--------|--------|
| Roughness (m) | 0.001 | 0.001 | 0.001 | 0.001 | 0.001 | 0.001 |
| Inner diameter (m) | 3 | 3 | 3 | 3 | 3 | 3 |
| Insulation thickness (m) | 0.6 | 0.6 | 0.6 | 0.6 | 0.6 | 0.6 |
| Air flow (kg/s) | 36 | 39 | 42.4 | 46 | 49.5 | 56.6 |
| Inlet temperature (°C) | 1000 | 1000 | 1000 | 1000 | 1000 | 1000 |
| Outlet temperature (°C) | 988 | 989 | 990 | 991 | 992 | 992.5 |
| Pressure drop (kPa) | 0.22 | 0.25 | 0.3 | 0.35 | 0.4 | 0.52 |
| Velocity (m/s) | 19 | 20 | 22 | 24 | 26 | 29 |
| Inner wall heat transfer coefficient (W/m ² K) | 12.5 | 13 | 14 | 15 | 16 | 18 |

Table 2.
Variation of mass flow—The same piping diameter and insulation.

| | Case 1 | Case 2a | Case 3a | Case 4a | Case 5a |
|--------------------------|--------|---------|---------|---------|---------|
| Roughness (m) | 0.001 | 0.001 | 0.001 | 0.001 | 0.001 |
| Inner diameter (m) | 3 | 3 | 3 | 3 | 3 |
| Insulation thickness (m) | 0.6 | 0.8 | 1 | 1.2 | 1.4 |
| Air flow (kg/s) | 36 | 36 | 36 | 36 | 36 |
| Pressure drop (kPa) | 0.22 | 0.22 | 0.22 | 0.22 | 0.22 |
| Inlet temperature (°C) | 1000 | 1000 | 1000 | 1000 | 1000 |
| Outlet temperature (°C) | 988 | 990.5 | 992 | 992.7 | 993 |

Table 3.
Variation of insulation thickness—The same mass flow and diameter.

and heat exchanger size by applying a regenerative heat exchange system (atmospheric heating, pressurized cooling).

1.2 The high-temperature thermocline thermal energy storage system upstream the gas turbine

The challenges of employing air as HTF are not only related to the HTF transport itself but also to the solar receiver design. Advanced power cycles are typically highly recuperative, since the average temperature of heat input to the cycle must be maintained high. This necessity implies that the HTF temperature interval in which heat is supplied to the cycle is typically small. In the case of the combined cycle, the temperature difference of the HTF is determined by the turbine inlet temperature and the compressor exit temperature (CET), which is a function of Brayton cycle pressure ratio. In the case of reheat, the HTF temperature difference is also determined by the reheat pressure level, i.e., the turbine exit temperature (TET) of the first turbine stage. Ideally, these two temperature levels (CET and TET) should be similar, in order to reduce losses when mixing the two streams (effective HTF return temperature). The effective HTF return temperature is the temperature at which the HTF leaves the power block after all parallel mass flow streams are merged (mixing temperature). At this temperature level, the HTF would then be recirculated to the solar receiver and again heated to the nominal

receiver outlet temperature, if an efficient and cost-effective receiver design was available for the case of atmospheric air.

However, in contrast to tubular receivers as used with molten salts, for example, the HTF recirculation, for the case of atmospheric air and open volumetric receivers, is not trivial. Previous research projects [29, 30] have targeted the design of open volumetric air receivers with air recirculation, however with limited success since only about 50% of the return air could be successfully recirculated [29]. Therefore, from a thermodynamic point of view, it would be more efficient to store the low-temperature heat of the return air for later use. Also, considering advanced power cycles with elevated HTF return temperatures (see the above), it would be too detrimental for the global performance, if relatively hot air was blown back to the receiver(s), especially when considering a multi-tower concept. It is clear that the operating temperature of air blowers must be as close as possible to ambient temperature, in order to keep a reasonable density.

Therefore, the present work considers the use of the return air heat in regenerative manner, applying a low-temperature air/rock thermocline TES (see **Figure 1**). The basic TES subunit consists of three packed beds, one high-temperature and two low-temperature units. Two low-temperature TES units are required because a packed bed cannot be charged and discharged at the same time. Hence, while discharging the TES system, the first low-temperature unit preheats ambient air until the nominal power cycle HTF return temperature is reached. Then, the preheated air enters the high-temperature storage unit where the air is heated to the nominal power cycle inlet temperature. Next, the HTF enters the power cycle, delivers part of its heat to the cycle, and finally charges the second low-temperature storage unit before being rejected to the atmosphere at a temperature very close to ambient conditions. During TES charging, only the high-temperature thermocline unit is being charged, that is, once the nominal receiver outlet temperature is approached at the bottom part of the high-temperature (HT) bed (cutoff condition), the TES system is fully charged. This also means that the low-temperature (LT) TES units need to be designed with larger bed heights (at same diameter and filling material characteristics) so that the blowers always operate close to ambient temperature and no heat is lost to the ambient. When upscaling the thermal storage capacity, several of such three bed subunits (1 HT TES + 2 LT TES) need to be applied. Additionally, in order to keep the system balanced, so that always one LT TES system is empty before the storage system is being discharged, one of the LT TES units needs to be discharged by boosting/powering the bottoming Rankine cycle. Note that the (dispatchable) boost operation is preferred over the direct boost during diurnal charging as the air mass flow is constant and does not depend on current solar irradiance (receiver temperature control). Therefore, the Rankine cycle can be run at constant load. Also, in order to keep the thermocline in the LT TES system balanced, its operation needs to be switched from time to time, so that not always the same LT TES unit is being charged by the HTF return stream. Having separate HT and LT TES units allows the application of temperature-specific materials for the packed bed as well as for the internal insulation of the tank, which allows to design the LT units much more economically.

The design of the packed beds would be equivalent to the system proposed in Refs. [23, 24].

Last but not the least, one remark needs to be given on how to operate the plant during the day. On the one hand, there is the possibility to only operate the power block during the night or only at times of high electricity prices, powering it via the TES only. In this case, direct solar operation is not implemented. On the other hand, if direct solar operation during the day is wanted in order to increase the capacity factor of the power block, two possibilities exist: (i) only the Rankine cycle is

operated during the day, which eliminates the need for a regenerative LT TES during the day, and also allows a reduced receiver operating temperature during the day, once the HT TES is full; (ii) the combined cycle is operated during the day, channeling the HTF return stream to the bottoming Rankine cycle, which significantly increases Rankine cycle output (i.e., its nominal power) and leads to reduced overall conversion efficiency, since it is not a true combined cycle. The operating principle of choice will depend on the specific electricity market.

1.3 The motivation for a reheated Brayton cycle and its application in the context of combined cycle power generation

As it is well known according to the principles of thermodynamics, reheat increases the average temperature of heat supply and thus increases the conversion efficiency from heat to mechanical work (Carnot). However, since a second heat input adds additional pressure losses, higher compressor pressure ratios are required to offset the performance penalty. This requirement is even more relevant for a solar-powered than an externally heated Brayton cycle. Reheated gas turbines have been already treated in previous works. The main motivations are (i) to keep the average temperature of heat supply high and (ii) to introduce an additional flexibility regarding turbine exit temperature (the heat recovery steam generator inlet temperature), despite high compressor pressure ratios [13, 31]. In particular, the expansion ratio of the second turbine stage can be specifically designed, so that the resulting TET optimizes the overall combined cycle performance. Note that the higher the heat recovery steam generator's inlet temperature is, the higher is the conversion efficiency of the bottoming cycle and vice versa. As proposed by Siros and Fernández-Campos [12], the reheat pressure level will be defined by a dimensionless parameter K (reheat ratio), which determines the ratio of pressure ratios of both turbine stages:

$$K = \frac{\text{pressure ratio of first stage}}{\text{pressure ratio of second stage}} = \frac{\frac{p_{t1i}}{p_{t1o}}}{\frac{p_{t2i}}{p_{t2o}}} = \frac{p_{t1i}}{p_{t1o}} \cdot \frac{p_{t2o}}{p_{t2i}} \quad (1)$$

Here, three considerations must be kept in mind:

- i. The reheat ratio K is a key parameter concerning Brayton cycle performance (on its own) as well as combined cycle performance; nevertheless, it has different optimums for the single cycle and the combined cycle. The lower the pressure ratio of the second turbine stage is, the higher the turbine exit temperature, i.e., HRSG inlet temperature, and thus the higher the efficiency of the bottoming Rankine cycle, but the lower the Brayton cycle performance. As shown in Ref. [10], solar combined cycle performance optimizes in the interval of $0.5 < K < 1.25$. The optimum value of K depends on concentration ratio, the corresponding optimum TIT, and HRSG efficiency. Note that Brayton single-cycle performance optimizes for values of K lower than in the case of combined cycle (see Ref. [32]).
- ii. Furthermore, the lower the pressure ratio of the second turbine stage is, the lower is the reheat pressure level and thus the bulkier and more expensive the second HTF-to-working-fluid heat exchanger will be. And the pressure drop would increase. Thus, there is clearly a lower practical limit for the second turbine stage's pressure ratio.

- iii. Having higher pressure ratios in the first turbine stage means lower TET at the first stage and thus corresponds to a lower return temperature of the TES medium (thus higher ΔT for the TES). Thus, higher pressure ratios in the first turbine stage are not only preferred in terms of Rankine cycle performance (see point (i)) but also regarding integration with thermal energy storage (second heat exchanger train).

In summary, a reheated Brayton cycle is absolutely interesting for the application of CSP as it allows fair conversion efficiencies despite low TITs. Reheat may increase solar-to-electric performance by up to about 2.7 percentage points [10]. Another argument for reheat is that the optimum cycle pressure ratio is much higher than in the case of a simple Brayton cycle. This means that the compressor exit temperature is higher, which allows for a higher effective HTF return temperature (low-temperature TES inlet temperature) and thus a more efficient boost of the bottoming Rankine cycle (see **Figure 1** dashed lines indicating periodical Rankine cycle boost in order to discharge the LT TES).

1.4 Motivations for multi-tower CSP plant arrangements

Basically, there are two options for multi-tower arrangements, (i) a simple multiple placement of identical solar field tower-receiver units, where each heliostat field concentrates solar radiation onto its corresponding receiver (tower) only or (ii) a special arrangement of multiple towers and heliostat fields, where heliostats of one field may point on different receivers (towers) as function of current solar position in order to optimize the overall optical efficiency. We propose to refer to the latter option “multi-tower multi-aiming” configuration, and to the first option “multi-tower assigned-aiming” configuration. The “multi-tower assigned-aiming” configuration is considered in this work.

Multi-tower arrangements with compact heliostat fields have significant advantages regarding solar field efficiency, atmospheric attenuation, and solar flux control at the receivers. This is because heliostats placed closer to the tower have higher optical efficiencies than those placed at the peripheral areas of the field [33]. Longer slant ranges, which may reach 1.5 km and more at large-capacity single-tower concepts [34, 35], already cause losses of up to 10% [36] purely considering atmospheric attenuation losses, not to mention spillage losses and increasingly challenging solar flux control. Thus, when upscaling a central receiver plant, there is a point where the heliostat field becomes simply too large. For this reason, a multi-tower approach is a promising way when going for very high capacity power tower plants, where Rankine cycle power blocks become more efficient and also cheaper per installed MW.

Additionally, the ongoing transformation from centralized conventional power generation to decentralized power supply with a high share of renewables calls for smaller modular units that can be easily adapted to the specific power demand. The general trend is expected to go towards more but lower capacity power generation units with lower capital risk and lower amount of initial investment [37]. However, so far in the case of CSP, current cost reduction trends are mainly driven by the increase of the nominal size of the main components (especially the power block) in order to reduce the cost of electricity production, as specific power cycle costs (\$/kWe) significantly reduce for large power ratings. This trend would change if we paid attention to the needs of the consumers and the changing, more and more decentralized electricity grid. Also, a modular design may reduce the perceived risk of the technology, giving the technology a better access to financing.

The principal problem in this context is that there is no power cycle available so far that is also cost-effective and efficient in smaller power classes. Typically, specific costs (\$/kWe) of gas turbines and Rankine cycles increase significantly for small power classes, and conversion efficiencies also decrease. If there was a cheap and efficient power cycle available in the power class below or around 10 MWe, solar power towers would be very compact plants, as the optical efficiency and consequently the solar-to-thermal efficiency are best for small solar fields. The only way in order to combine (i) good solar-to-thermal efficiency and (ii) an efficient power cycle (i.e., to maximize solar-to-electric energy conversion) is the application of multi-tower power plant concepts.

2. Cost review of power plant components

In order to perform a serious techno-economic study, the fundamental step is to collect realistic cost estimates for all power plant components. Therefore, a detailed literature search has been conducted collecting available cost data and also comparing them in order to guarantee consistency. All cost data given in this section has been converted into USD 2018 (inflation-adjusted).

2.1 High-temperature heat exchanger costs for powering the topping Brayton cycle externally

The most critical component of the proposed power plant concept (**Figure 1**) is the needed high-temperature gas-gas heat exchanger in order to power the topping Brayton cycle externally. As the coefficient of heat transfer on the atmospheric air side is very limited, the design is expected to be very bulky, since a large area of heat transfer is needed. In principal, a shell-and-tube heat exchanger design [11] is expected, having the pressurized air stream coming from the Brayton cycle's compressor on the tube side and the heating air stream at ambient pressure (coming from the TES) on the shell side. This type of heat exchanger will be similar to a heat recovery steam generator. Alternatively, and subject of this work, a regenerative heat exchange system working under atmospheric charging and pressurized discharging conditions can be applied [38] (see **Figure 2**), providing better heat exchange effectiveness. Clearly, the vessel size of this regenerative heat exchange system is limited due to the pressurization process, which requires several two-vessel subunits (such as shown in **Figure 2**) in parallel depending on the power rating. The second reason for several two-vessel subunits in parallel is the requirement for continuous thermal power transfer (while one system is pressurized/depressurized, the parallel systems need to take over). Thus, one disadvantage with respect to conventional heat exchangers is the higher complexity, as besides several parallel systems, high-temperature valves and piping are required for managing the pressurization/depressurization process. Furthermore, the pressurization process requires a certain amount of work, i.e., represents an additional parasitic consumption. This disadvantage needs to be offset by higher heat exchange effectiveness and reduced heat exchanger size (with respect to the conventional shell-and-tube layout). It is clear that this innovative regenerative system must have costs that are in the same order of magnitude as conventional heat exchanger designs in order to remain cost competitive. Here, cost figures published by Ilett and Lawn [39] are used. Calculating the cost difference between conventional combined cycle plants and externally fired ones results in a specific heat exchanger cost target of 64 kUSD per kg/s of air flow (topping Brayton cycle compressor air flow).

2.2 Gas turbine costs

The costs of the turbo machinery (compressor, turbine and turbo generator) are estimated as function of electric power output based on cost figures available in the open literature. Here it is important to capture the cost dependency on turbomachinery size, as smaller engines have higher specific costs (USD/kWe) than larger ones. Gas turbine costs are issued on a yearly basis by Gas Turbine World [40]. They propose a best fit curve, mentioning a $\pm 10\%$ accuracy for gas turbine ratings ranging from 1 to 500 MWe. The investment cost of the turbo machinery IC_{GT} in USD (2018) is given as function of electric output power P_{eGT} in kW in Eq. (2):

$$IC_{GT} = (9650 \cdot P_{eGT}^{-0.3}) \cdot P_{eGT} = 9650 \cdot P_{eGT}^{0.7} \quad (2)$$

2.3 Heat recovery steam generator (HRSG) costs

In order to obtain a reliable cost relationship for the heat recovery steam generator, the cost correlations published by Roosen et al. [41] and Silveira and Tuna [42] have been compared and agree very well once inflation-adjusted. Based on the correlation presented in Ref. [42], the following cost equation has been developed (in USD 2018), which only depends on heat duty \dot{Q} (kW), air inlet temperature $T_{air\ in}$, stack temperature $T_{air\ out}$, and air mass flow \dot{m}_{air} (kg/s):

$$IC_{HRSG} = 1.37 \cdot \left[4745 \cdot \left(\frac{\dot{Q}}{\ln(T_{air\ in} - T_{air\ out})} \right)^{0.8} + 2195 \cdot \dot{m}_{air} \right] \quad (3)$$

2.4 Steam turbine and remaining Rankine cycle component costs

Also steam turbine cost relationships published by Roosen et al. [41] and Silveira and Tuna [42] agree very well and, once inflation-adjusted, are also consistent with recent quotes requested by the authors. The adapted correlation (from Ref. [42]) is as follows:

$$IC_{ST} = 8220 \cdot P_{eST}^{0.7} \quad (4)$$

According to recent quotes, the cost estimate given by Eq. (4) may also include remaining Rankine cycle components, such as dry air-cooled condenser, feed water pumps, and deaerator. Finally, the above presented cost relationships have additionally been checked for consistency against Refs. [39, 43].

2.5 Heliostat field, tower, solar receiver, TES, and piping costs

Heliostat field costs are taken from Pfahl et al. [44], assuming 75 USD/m². This cost figure seems to be a realistic engineering target for heliostat designs that are optimized for mass production. The total heliostat field investment cost is obtained by multiplying the specific cost by the total solar field reflective area.

For the optimization process of the proposed multi-tower plant concept, small-to medium-sized fields are interesting, having tower heights in the range between 50 and 150 m. These tower heights are typical for wind turbines, and cost estimates for wind turbine towers should be applicable for solar power towers too, however considering larger tower diameters depending on needed piping diameter and receiver aperture size. Possible construction types for solar thermal power towers are either concrete type or metallic lattice type.

The following tower cost correlation has been established based on data given in Ref. [45] as function of tower height h_{tower} (m). The result, IC_{tower} , is the complete investment cost of the tower construction plus foundations and transport in M USD (2018), taking into account larger diameter towers providing enough space for the needed hot air piping as well as the receiver. Note that the valid height range for Eq. (5) is from 50 to 200 m:

$$IC_{tower} = 1.50227 - 0.00879597 \cdot h_{tower} + 0.000189709 \cdot h_{tower}^2 \quad (5)$$

The cost estimate of the solar receiver has been based on the CAPTURE receiver prototype (≈ 300 kW_{th}) costs, taking into account possible cost reductions when manufacturing the receiver up-scaled and in higher numbers commercially. The costs have been calculated per square meter of aperture area and result in 30 kUSD/m² for receiver aperture areas below 130 m², 50 kUSD/m² for receiver aperture areas until 400 m², and 100 kUSD/m² for bigger receiver aperture areas. The total aperture size of the receiver is an important factor as the receiver base structure (metallic + insulation) that supports modular ceramic absorber structures (cups + foams) as well as the air duct system becomes more complex and expensive the bigger the receiver is.

The costs of air/rock or air/ceramic thermocline packed-bed thermal energy storage can be assumed to be 20 USD/kWh_{th} [25]. However, in the case of the specific plant arrangement shown in **Figure 1**, the TES costs are higher since two low-temperature TES units are required for each high-temperature TES unit (regenerative use of return air heat). This approach is assumed to double the specific cost per kWh_{th}, resulting in 40 USD/kWh_{th} for the combined cycle option, only. Note that in the case of the Rankine single-cycle (benchmarking) configuration, the low-temperature TES units are not needed and the lower cost assumption applies.

The cost of internally insulated high-temperature piping has been assumed to be 800 USD per meter piping and per square meter flow cross section. It must be noted that the air speed in the air piping system must be kept reasonably low (≈ 20 m/s) in order to achieve acceptable pressure drop and thus blower power consumption.

The cost of blowers for circulation of air in the atmospheric circuit (blowers operate at ambient temperature) is assumed to be 3 kUSD per air volume flow (m³/s). This cost assumption is based on several quotes requested by the authors.

Last but not the least, the yearly operations and maintenance (O&M) costs are assumed to be 1.5% of the total plant investment cost [3].

2.6 Levelized cost of electricity (LCOE) calculation

In the literature, the LCOE is an established figure for evaluating purely the economic lifetime energy production and its related lifetime costs, without taking into account revenues [46]. As revenues, i.e., feed-in tariffs, depend strongly on the country, the LCOE is therefore a relatively market-neutral figure and also allows to compare alternative technologies with different scales of investment or operating time [47]. Nevertheless, the LCOE depends on country-dependent parameters such as available solar resource, capital cost, and O&M costs, which must be taken into account in a serious technology benchmarking process. The general understanding of the LCOE in the literature [46, 48] is the total lifetime cost of the plant (engineering + construction + operation + maintenance + capital costs) divided by the lifetime electricity generation (total electric energy produced). Its unit is therefore cost per energy, i.e., USD/kWh. A particular point in the definition of the LCOE is that all costs incurred during the project lifetime are discounted back to the base

year, i.e., their net present value (NPV) is taken into account [47]. Thus, according to Ref. [47], the LCOE can be calculated as given by Eq. (6). Note that C_n is the incurred cost in period n (engineering, construction, operation, maintenance, cost of capital), Q_n is the energy output in year n , d is the discount rate, and N is the total analysis period in years (power plant lifetime):

$$LCOE = \frac{\sum_{n=0}^N \frac{C_n}{(1+d)^n}}{\sum_{n=1}^N \frac{Q_n}{(1+d)^n}} \quad (6)$$

Also note that the applied discount rate should be the “real” discount rate, taking into account the inflation rate. A real discount rate of 3% is used in this work. The cost of capital for financing a CSP project is assumed to be 5% p.a. Power plant operating time is assumed to be 30 years (SEGS plants in the USA are in operation since the 1980s).

3. Power plant performance modeling

The power plant performance modeling is done as outlined in Ref. [10]. In particular, the solar receiver performance is estimated according to Ref. [49], using the detailed 1-D model to establish a receiver performance table as function of receiver operating temperature and incident solar flux. The topping Brayton cycle is modeled applying the isentropic relationships for air as ideal gas and choosing power class-dependent isentropic efficiencies. The bottoming Rankine cycle performance has been estimated applying state-of-the-art power cycle simulation software [43] and generating performance tables as function of HRSG inlet temperature and ambient temperature [10], suitable for annual yield simulations. The annual plant performance parameters (i.e., electricity yield, annual solar-to-electric efficiency) have been obtained running annual energy yield simulations using a typical meteorological year for Seville, Spain. The operating strategy is chosen such that the power block always operates under rated conditions (corresponding TES system charging/discharging) apart from start-up and shutdown periods.

3.1 Turbo machinery isentropic efficiencies as function of electric power output

As commonly known, the efficiency of turbomachinery is a function of power rating, i.e., the higher the output power, the higher is also the efficiency. Conversely, smaller engines have lower efficiencies. This is principally due to size-specific impacts of aerodynamic losses. For example, the turbine blade tip clearance (i.e., the radial distance between the blade tip of an axial compressor or turbine and the containment structure) is a major contributing factor to gas path sealing and can significantly affect engine efficiency [50]. The tip-leakage flow contributes negatively to the turbine performance and accounts for approximately one third of the total aerodynamic loss [51]. The bigger the engine, the smaller is the tip clearance with respect to the overall blade length and thus the higher is the efficiency.

It is clear that the size-dependent relationship of the turbomachinery’s efficiency needs to be taken into account in the techno-economic optimization. In order to do so, relationships and performance tables have been established that consider efficiency as a function of output power, for both the topping Brayton cycle and for the bottoming Rankine cycle. For detailed information, the interested reader is referred to the corresponding public CAPTURE project [38] deliverable D1.4 “CAPTURE concept specifications and optimization.”

4. Parametric benchmarking of power plant configurations: Combined cycle (CC) vs. Rankine single cycle (RC)

The principal objective of this section is to benchmark the techno-economic optimum of the CC plant against that of a conventional single-cycle Rankine steam plant with the same receiver and TES technology (see **Figure 3**). This will allow a fair assessment of the solar-powered combined cycle performance.

In order to analyze the impact of different solar field sizes and number of tower-solar-field modules, five solar field base modules (A, B, C, D, and E) have been selected (see **Table 1**, **Figures 4** and **5**). The applied solar field layout pattern is DELSOL [52], and solar field efficiency matrices can be obtained from CAPTURE project deliverable D1.4. The base modules have been chosen such that different multiples achieve the same solar power class. For example, 9 B modules have the same nominal solar power as 3 C modules or 1 D module, i.e., 153 MW solar at the receiver(s). In this way, a direct comparison of conventional single-tower and multi-tower configurations can be achieved, giving also emphasis on the impact of total electric power of the plant. The general expected trends are that:

- i. Smaller solar fields have higher optical efficiency.
- ii. By arranging multiple solar field units as array, the optical efficiency for a given total solar power is improved; however, there is a point where HTF transport and additional tower and piping investment become too detrimental and the global performance is not better than that of a single-tower arrangement.
- iii. Despite of much better optical efficiency of compact multi-tower arrangements, the considerable decrease in conversion efficiency of small power cycles, as well as elevated specific costs, generally makes small CSP plants economically unfeasible.

For each of the 19 configurations as indicated in **Table 1** (3 A to 9 A, 1 B to 9 B, 1 C to 9 C, 1 D to 4 D, and 1 E), the power plant performance models (combined cycle and single-cycle Rankine) have been run estimating the yearly energy yield and in consequence the resulting LCOE. The results are indicated in **Table 1** as well as in **Figure 6**. Note that the solar multiple (SM) and the TES capacity (hours of storage) have been optimized, i.e., obtaining the minimum LCOE at a solar multiple of about 2.3 and 10 full load hours of TES. The optimum solar multiple and TES capacity are typically only functions of geographic location and solar resource. When looking at **Table 1**, the first important trend that can be observed across all columns (all solar

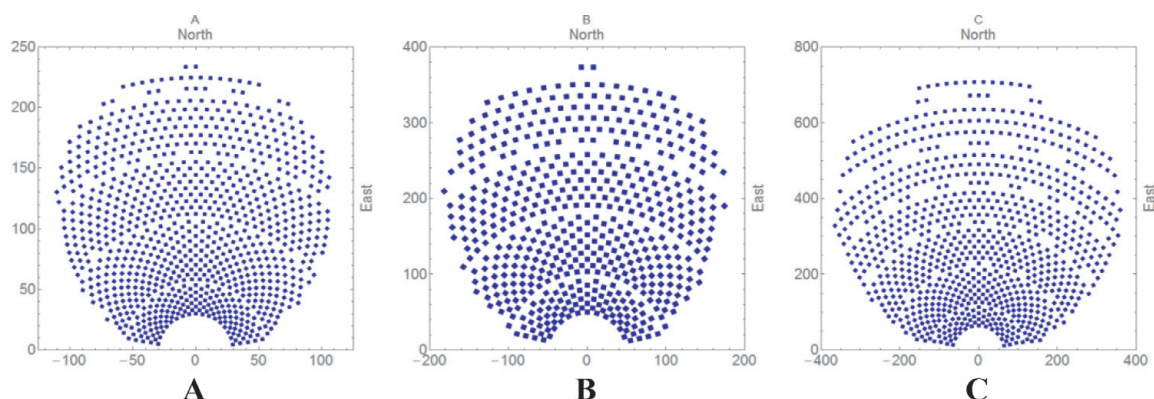


Figure 4.
Solar field base module types A, B, and C (solar field dimensions given in meters).

field base modules) is that when moving to a higher solar power class, the LCOE decreases. This is principally due to the fact that when moving to higher nominal power of the power block, the turbomachinery becomes more efficient and also the specific power block costs (\$/kWe) reduce. This is the reason why commercial CSP projects have increased in size recently. However, when increasing the nominal solar power of a multi-tower arrangement (i.e., increasing the number of towers) above a certain threshold, the needed piping for HTF transport becomes an issue (investment, thermal losses, and pumping power); hence LCOE increases again (see configurations 9 C, 3 D, and 4 D). The second important trend that can be observed is that the single-tower configuration is only more competitive than a multi-tower configuration (of the same nominal solar power) below about 153 MW total nominal solar power. Above this threshold, the increase in investment (more towers, longer piping) and additional HTF transport power consumption are offset by the positive effect of higher optical efficiency of the more compact solar field base modules and smaller receiver aperture areas (cost advantage).

The most competitive (lowest LCOE) combined cycle power plant configuration is 6 C with a LCOE of 12.6 c\$/kWh. However, the most competitive Rankine single-cycle plant configuration (also of type 6 C) achieves an LCOE of 11.5 c\$/kWh. Thus, it is concluded that the combined cycle plant is despite its higher solar-to-electric conversion efficiency more expensive than the much simpler but less efficient single-cycle Rankine option. However, when observing **Table 1**, the difference in LCOE becomes smaller for smaller power classes, and the CC plant achieves better performance at 34 MW (and lower) total solar power. This is an effect of different power cycle efficiency decrease at small power classes, i.e., the combined cycle stays relatively more efficient than the Rankine single cycle configuration, which pays off for very small plant configurations. For this reason, the combined cycle seems to be

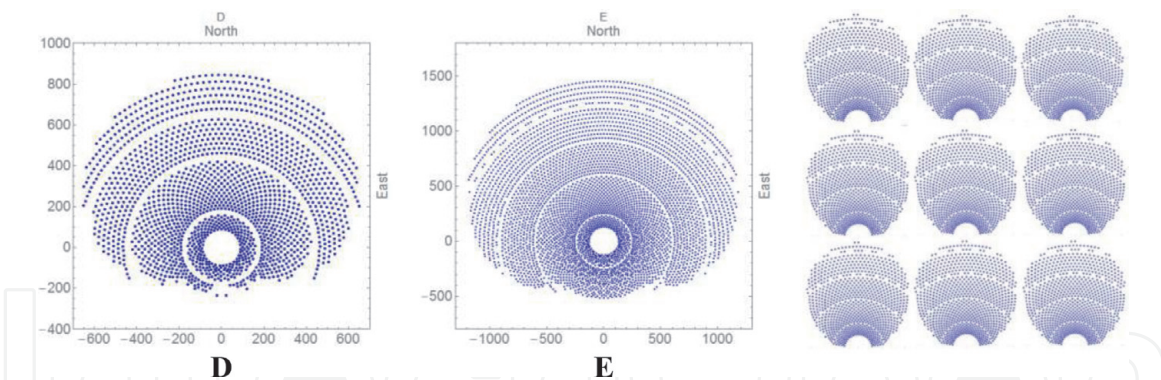


Figure 5. Solar field base module types D and E (solar field dimensions given in meters). Multi-tower configuration 9 A (right-hand side).

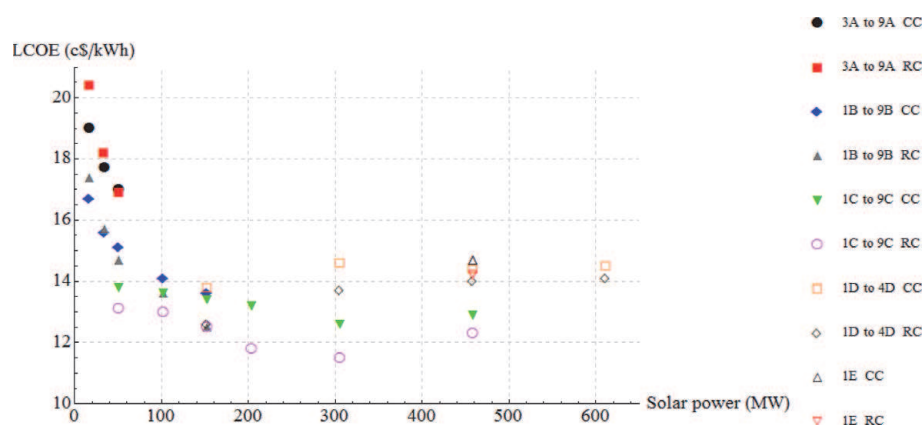


Figure 6. LCOE as function of nominal solar power incident at receiver(s) and plant configuration (see also **Table 1**).

| Parameter (unit) | 6C CC | 6C RC | 2B CC | 2B RC |
|---|---------------------|------------|--------------------|------------|
| Number of towers (–) | 6 | 6 | 2 | 2 |
| Nominal solar power per tower (MW) | 51 | 51 | 17 | 17 |
| Total nominal solar power (MW) | 306 | 306 | 34 | 34 |
| Receiver thermal efficiency (–)/operating temperature (°C) | 0.75/1050 | 0.81/800 | 0.75/1050 | 0.81/800 |
| Solar-to-electric peak efficiency (–) | 0.296 | 0.25 | 0.27 | 0.209 |
| Solar-to-electric annual mean efficiency (–) | 0.202 | 0.195 | 0.182 | 0.152 |
| Solar multiple (–) | 2.3 | 2.3 | 2.3 | 2.3 |
| Power cycle nominal power (MWe) | 50 | 45 | 4.9 | 3.7 |
| Reheated GT nominal power (MWe) | 28 | — | 3 | — |
| Rankine cycle nominal power (MWe) | 22 | 45 | 1.9 | 3.7 |
| Power cycle annual mean conversion efficiency: CC/GT/RC (–) | 0.496/0.288 / 0.355 | —/—/ 0.388 | 0.434/0.268/ 0.277 | —/—/ 0.295 |
| TES thermal capacity (MWh) | 981 | 1194 | 109 | 131.3 |
| Yearly electricity yield (GWh) | 161.6 | 156.8 | 15.6 | 13 |
| Total plant cost (M USD) | 175.35 | 154.55 | 20.93 | 17.51 |
| Specific plant costs (USD/kWe) | 3507 | 3434 | 4271 | 4732 |
| Specific power cycle costs (USD/kWe) | 849 | 678 | 1473 | 1423 |
| LCOE (c\$/kWh) | 12.6 | 11.5 | 15.6 | 15.7 |

Table 4.
Power plant specifications of plant type 6 C and 2 B.

only attractive for very small power tower plants (below 5 MWe). Although gas turbines can be scaled down quite well having reasonable performance at small power classes, this is not the case for Rankine steam cycles. Hence, when thinking of very small (i.e., “micro”) combined cycles, the application of the organic Rankine cycle (ORC) as bottoming power cycle should be considered. This concept could be attractive for small and modular CSP central receiver plants for “electricity islands,” i.e., small remote grids, where electricity price is very high.

Table 4 shows the most important parameters of power plant configurations 6 C and 2 B. For plant configuration 6 C, it can be seen that although the combined cycle option achieves a higher solar-to-electric conversion efficiency, the increased plant complexity and thus its higher investment are not compensated by the increase in electricity yield. The combined cycle becomes cost competitive only at smaller power classes (see results for plant configuration 2 B in **Table 4**).

5. Conclusions

The parametric study shows that the multi-tower configuration has a techno-economic advantage with respect to the conventional single-tower arrangement above a total nominal solar power level of about 150 MW. The most competitive power plant configuration is of type 6 C. The combined cycle plant configuration reaches an LCOE of 12.6 c\$/kWh, whereas the Rankine single-cycle power plant layout achieves 11.5 c\$/kWh. Hence, the CC configuration has despite its higher solar-to-electric conversion efficiency a higher LCOE. The gain in electricity yield is

not enough to outweigh the higher investment costs of the more complex CC plant layout. The CC configuration seems to be competitive only at smaller power classes. It must be said that all cost assumptions have inherent uncertainty, which makes a final conclusion regarding the best power plant layout very difficult. It is however clear that compact power plant arrangements (A, B, C options) are the preferred choice for the CAPTURE power plant concept that applies atmospheric air as HTF, as large diameter piping (low air speeds are mandatory) becomes an issue at higher power classes, not only in terms of investment but also in terms of thermal inertia and losses. Therefore, it is very likely that in practical terms, a single-tower plant configuration will be the best choice when applying atmospheric air as HTF, as differences in LCOE are small. Furthermore, compact power tower plants have clear advantages regarding solar flux control, and also concerning total investment as financing is usually easier to obtain for smaller projects.

Finally, in order to make the CC attractive for CSP plants, the following challenges remain: (i) the efficiency of the solar receiver at relevant operating temperatures ($\approx 1000^{\circ}\text{C}$) must be increased, and in particular innovative and economically competitive solar receiver designs are sought that allow long-term operation ($\approx 25\text{--}30$ years) at very high solar flux densities, i.e. high concentration ratios; (ii) with regard to the investigated power plant layout, i.e. when using an open volumetric air receiver and atmospheric air as HTF, it is crucial to design a very economical high-temperature air–air heat exchanger train for powering the topping gas turbine externally.

Acknowledgements

This work has received funding from the European Union's Horizon 2020 research and innovation program under the grant agreement No 640905.

Author details

Fritz Zaversky^{1*}, Iñigo Les¹, Marcelino Sánchez¹, Benoît Valentin², Jean-Florian Brau², Frédéric Siros², Jonathon McGuire³ and Flavien Berard³

¹ National Renewable Energy Center (CENER), Solar Thermal Energy Department, Navarra, Spain

² EDF – R&D, Chatou, France

³ Bluebox Energy Ltd., Hants, United Kingdom

*Address all correspondence to: fzaversky@cener.com

IntechOpen

© 2019 The Author(s). Licensee IntechOpen. This chapter is distributed under the terms of the Creative Commons Attribution License (<http://creativecommons.org/licenses/by/3.0>), which permits unrestricted use, distribution, and reproduction in any medium, provided the original work is properly cited. 

References

- [1] Abbott D. Keeping the energy debate clean: How do we supply the world's energy needs? *Proceedings of the IEEE*. 2010;**98**:42-66
- [2] ESTELA. *The Value of Solar Thermal Electricity - Cost vs. Value Approach*, ESTELA - European Solar Thermal Electricity Association, Brussels, Belgium; 2016
- [3] Lilliestam J, Pitz-Paal R. Concentrating solar power for less than USD 0.07 per kWh: Finally the breakthrough? *Renewable Energy Focus*. 2018;**26**:17-21
- [4] Ho CK. Advances in central receivers for concentrating solar applications. *Solar Energy*. 2017;**152**:38-56
- [5] Ganapathy V. *Industrial Boilers and Heat Recovery Steam Generators - Design, Applications, and Calculations*. New York, USA: Marcel Dekker, Inc.; 2003
- [6] Dunham MT, Iverson BD. High-efficiency thermodynamic power cycles for concentrated solar power systems. *Renewable and Sustainable Energy Reviews*. 2014;**30**:758-770
- [7] Stein WH, Buck R. Advanced power cycles for concentrated solar power. *Solar Energy*. 2017;**152**:91-105
- [8] Miller J. The combined cycle and variations that use HRSGs. In: Eriksen VL, editor. *Heat Recovery Steam Generator Technology*. Duxford, United Kingdom: Woodhead Publishing; 2017. pp. 17-43
- [9] Fraidenraich N, Gordon JM, Tiba C. Optimization of gas-turbine combined cycles for solar energy and alternative-fuel power generation. *Solar Energy*. 1992;**48**:301-307
- [10] Zaversky F, Les I, Sorbet P, Sanchez M, Valentin B, Brau J-F, et al. The challenge of solar powered combined cycles - providing dispatchability and increasing efficiency by integrating the open volumetric air receiver technology. *Energy*; 2020
- [11] Al-attab KA, Zainal ZA. Externally fired gas turbine technology: A review. *Applied Energy*. 2015;**138**:474-487
- [12] Siros F, Fernández Campos G. Optimisation of a low-TIT combined cycle gas turbine with application to new generation solar thermal power plants. In: *ASME 2017 Turbo Expo*. Charlotte, NC, USA; ASME; 2017. pp. V003T006A038
- [13] Polyzakis AL, Koroneos C, Xydis G. Optimum gas turbine cycle for combined cycle power plant. *Energy Conversion and Management*. 2008;**49**: 551-563
- [14] Becker M. *GAST - The Gas Cooled Solar Tower Technology Program*. Berlin Heidelberg, Germany: Springer Verlag; 1989
- [15] Ávila-Marín AL. Volumetric receivers in solar thermal power plants with central receiver system technology: A review. *Solar Energy*. 2011;**85**:891-910
- [16] Grange B, Dalet C, Falcoz Q, Ferrière A, Flamant G. Impact of thermal energy storage integration on the performance of a hybrid solar gas-turbine power plant. *Applied Thermal Engineering*. 2016;**105**:266-275
- [17] Korzynietz R, Brioso JA, del Río A, Quero M, Gallas M, Uhlig R, et al. Solugas – comprehensive analysis of the solar hybrid Brayton plant. *Solar Energy*. 2016;**135**:578-589
- [18] Puppe M, Giuliano S, Krüger M, Lammel O, Buck R, Boje S, et al. Hybrid high solar share gas turbine systems

with innovative gas turbine cycles.
Energy Procedia. 2015;**69**:1393-1403

[19] Hennecke K, Schwarzbözl P, Alexopoulos S, Götsche J, Hoffschmidt B, Beuter M, et al. Solar Power Tower Jülich - the First Test and Demonstration Plant for Open Volumetric Receiver Technology in Germany. Las Vegas, USA: SolarPACES; 2008

[20] Kwakernaak H, Tijssen P, Strijbos RCW. Optimal operation of blast furnace stoves. Automatica. 1970;**6**:33-40

[21] Hausen H. Berechnung der Wärmeübertragung in Regeneratoren bei zeitlich veränderlichem Mengenstrom. International Journal of Heat and Mass Transfer. 1970;**13**: 1753-1766

[22] Hennecke K, Hoffschmidt B, Koll G, Schwarzbözl P, Götsche J, Beuter M, et al. The Solar Power Tower Jülich - a Solar Thermal Power Plant for Test and Demonstration of Air Receiver Technology. Beijing, China: ISES World Congress; 2007

[23] Zanganeh G, Pedretti A, Zavattoni S, Barbato M, Steinfeld A. Packed-bed thermal storage for concentrated solar power – Pilot-scale demonstration and industrial-scale design. Solar Energy. 2012;**86**: 3084-3098

[24] Zanganeh G, Pedretti A, Haselbacher A, Steinfeld A. Design of packed bed thermal energy storage systems for high-temperature industrial process heat. Applied Energy. 2015;**137**: 812-822

[25] ALACAES-SA, ALACAES - Creating Sustainable Energy Solutions for a Brighter Future, Lugano, Switzerland; 2017. Available from: <https://alacaes.com/>

[26] Fricker HW. Regenerative thermal storage in atmospheric air system solar power plants. Energy. 2004;**29**:871-881

[27] Hänchen M, Brückner S, Steinfeld A. High-temperature thermal storage using a packed bed of rocks - heat transfer analysis and experimental validation. Applied Thermal Engineering. 2011;**31**:1798-1806

[28] Moody LF. Friction factors for pipe flow. Transactions of the ASME. 1944;**66**:671-684

[29] Hoffschmidt B, Téllez FM, Valverde A, Fernández J, Fernández V. Performance evaluation of the 200-kWth HiTRec-II open volumetric air receiver. Journal of Solar Energy Engineering. 2003;**125**:87-94

[30] Téllez F. Thermal Performance Evaluation of the 200kWth “SolAir” Volumetric Solar Receiver. Madrid, Spain: CIEMAT-PSA; 2003

[31] Doligalski A, Sanchez de Leon L, Zachos PK, Pachidis V. Assessing the Potential of Gas-Recuperation in Reheated Gas Turbines Within Combined Gas-Steam Power Plants; 2014, V03AT07A031

[32] Sheikhbeigi B, Ghofrani MB. Thermodynamic and environmental consideration of advanced gas turbine cycles with reheat and recuperator. International Journal of Environmental Science and Technology. 2007;**4**: 253-262

[33] Sánchez M, Romero M. Methodology for generation of heliostat field layout in central receiver systems based on yearly normalized energy surfaces. Solar Energy. 2006;**80**:861-874

[34] Sment J, Ho CK, Moya AC, Ghanbari CM. Long-distance flux mapping using low-cost collimated pyranometers. Solar Energy. 2014;**100**: 76-83

- [35] Ballestrín J, Marzo A. Solar radiation attenuation in solar tower plants. *Solar Energy*. 2012;**86**:388-392
- [36] Sengupta M, Wagner M. Atmospheric Attenuation in Central Receiver Systems from DNI Measurements. Denver, Colorado, USA: ASES National Solar Conference; 2012
- [37] Romero M, Marcos MAJ, Téllez FM, Blanco M, Fernández V, Baonza F, et al. Distributed power from solar tower systems: A MIUS approach. *Solar Energy*. 1999;**67**:249-264
- [38] CENER, Horizon 2020 Research Project “CAPTURE - Competitive Solar Power Towers” - Grant Agreement Number 640905. 2015. Available from: www.capture-solar-energy.eu/
- [39] Ilett T, Lawn CJ. Thermodynamic and economic analysis of advanced and externally fired gas turbine cycles. *Proceedings of the Institution of Mechanical Engineers, Part A: Journal of Power and Energy*. 2010;**224**:901-915
- [40] Isles J. *Gas Turbine World - 2018 GTW Handbook*. Southport, CT, USA: Pequot Publishing Inc.; 2018
- [41] Roosen P, Uhlenbruck S, Lucas K. Pareto optimization of a combined cycle power system as a decision support tool for trading off investment vs. operating costs. *International Journal of Thermal Sciences*. 2003;**42**:553-560
- [42] Silveira JL, Tuna CE. Thermo-economic analysis method for optimization of combined heat and power systems. Part I. *Progress in Energy and Combustion Science*. 2003;**29**:479-485
- [43] Thermoflow-Inc., GT PRO - Gas turbine combined cycle design program to create cycle heat balance and physical equipment needed to realize it. 2018. Available from: http://www.thermoflow.com/combinedcycle_GTP.html [Accessed: 27 July 2018]
- [44] Pfahl A, Coventry J, Röger M, Wolfertstetter F, Vásquez-Arango JF, Gross F, et al. Progress in heliostat development. *Solar Energy*. 2017;**152**: 3-37
- [45] Engström S, Lyrner T, Hassanzadeh M, Stalin T, Johansson J. *Tall Towers for Large Wind Turbines, Elforsk - Electricity and Power Production*. Stockholm, Sweden: Elforsk, Electricity and Power Production; 2010
- [46] Cartelle Barros JJ, Lara Coira M, de la Cruz López MP, del Caño Gochi A. Probabilistic life-cycle cost analysis for renewable and non-renewable power plants. *Energy*. 2016;**112**:774-787
- [47] Short W, Packey DJ, Holt T. *A Manual for the Economic Evaluation of Energy Efficiency and Renewable Energy Technologies* NREL/TP-462-5173. National Renewable Energy Laboratory; 1995. Available from: <https://www.nrel.gov/docs/legosti/old/5173.pdf>
- [48] IRENA, *Renewable Energy technologies: Cost Analysis Series - Concentrating Solar Power*, IRENA - International Renewable Energy Agency. 2012. Available from: www.irena.org/Publications
- [49] Zaversky F, Aldaz L, Sánchez M, Ávila-Marín AL, Roldán MI, Fernández-Reche J, et al. Numerical and experimental evaluation and optimization of ceramic foam as solar absorber – Single-layer vs multi-layer configurations. *Applied Energy*. 2018;**210**:351-375
- [50] Chapman JW, Kratz J, Guo TH, Litt J. *Integrated Turbine Tip Clearance and Gas Turbine Engine Simulation*, NASA/TM—2016-219146. Cleveland, Ohio, USA: National Aeronautics and Space Administration - NASA; 2016
- [51] Denton JD. The 1993 IGTI scholar lecture: Loss mechanisms in

Turbomachines. Journal of
Turbomachinery. 1993;**115**:621-656

[52] Kistler BL. A User's Manual for
DELSOL3: A Computer Code for
Calculating the Optical Performance
and Optimal System Design for Solar
thermal Central Receiver Plants, Sandia
National Laboratories, Albuquerque,
New Mexico and Livermore, California;
1986

IntechOpen

IntechOpen